

MRTNet: Multi-Resolution Temporal Network for Video Sentence Grounding

Wei Ji

National University of Singapore
Singapore
weiji0523@gmail.com

Long Chen

Columbia University
USA

Yinwei Wei

National University of Singapore
Singapore
weiyinwei@hotmail.com

Yiming Wu

The University of Sydney
Australia
weiyinwei@hotmail.com

Tat-Seng Chua

National University of Singapore
Singapore
dcscts@nus.edu.sg

ABSTRACT

Given an untrimmed video and natural language query, video sentence grounding aims to localize the target temporal moment in the video. Existing methods mainly tackle this task by matching and aligning semantics of the descriptive sentence and video segments on a single temporal resolution, while neglecting the temporal consistency of video content in different resolutions. In this work, we propose a novel multi-resolution temporal video sentence grounding network: MRTNet, which consists of a multi-modal feature encoder, a Multi-Resolution Temporal (MRT) module, and a predictor module. MRT module is an encoder-decoder network, and output features in the decoder part are in conjunction with Transformers to predict the final start and end timestamps. Particularly, our MRT module is hot-pluggable, which means it can be seamlessly incorporated into any anchor-free models. Besides, we utilize a hybrid loss to supervise cross-modal features in MRT module for more accurate grounding in three scales: frame-level, clip-level and sequence-level. Extensive experiments on three prevalent datasets have shown the effectiveness of MRTNet.

CCS CONCEPTS

- Computing methodologies → Visual content-based indexing and retrieval.

KEYWORDS

video sentence grounding, temporal resolution, cross-modal

1 INTRODUCTION

Video sentence grounding aims to localize the temporal moments from the untrimmed video corresponding to the given descriptive language query. As an important visual-language task, video sentence grounding involves both computer vision (CV) and natural language processing (NLP) techniques, and is beneficial to numerous down-stream video understanding tasks, such as video dialog [7], video relationship detection [18, 30, 31], and video question answering [19, 40, 56], *etc.* Clearly, the cross-modal semantic consistency is essential for video sentence grounding.

Prior works primarily treat video sentence grounding as a ranking problem, *i.e.*, applying a multi-modal matching architecture to find the best matching moment for the given language query, which can be treated as proposal-based methods. Recently, some works explore

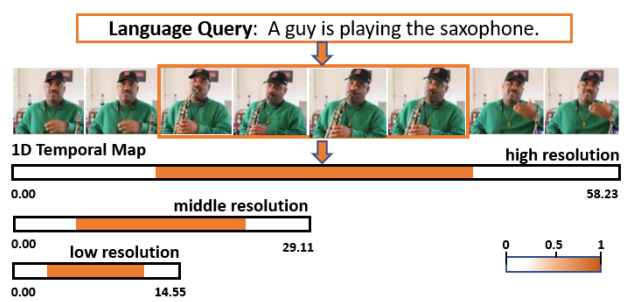


Figure 1: An illustration of localizing a temporal moment in an untrimmed video by a language query. The 1D temporal map shows the response area in the whole video sequence, according to the language query. As shown above, if video is compressed with different sampling rates, these 1D temporal maps will display in high, middle, and low resolutions, while the relative locations of target regions stay unchanged.

the cross-modal matching between video and query, and then directly regress the temporal locations of target moment, which is classified as proposal-free methods. Commonly, the structure of current proposal-free video language grounding methods mainly includes these modules: visual and language encoders module, multi-modal attention module, and predictor module. The results calculated by the predictor module heavily rely on the multi-modal features with attention. However, these methods neglect the temporal consistency of video data in multi-resolutions, which is beneficial for better video feature representation.

In this paper, we try to deal with the video sentence grounding task from another perspective: In the 1D temporal dimension, the target range in video can be treated as the foreground region, and the rest of the video is viewed as the background. The essence of video sentence grounding is to localize the maximum response area in 1D temporal range according to the descriptive query. As we known, attention map can also be treated as the maximum response area in the temporal dimension. Hence, context information in the whole video is crucial for locating the accurate boundaries of temporal segments.

On the basis of the previous network design, we propose a plug-and-play module to constrains the temporal consistency of video

in different resolutions. In the module design, we aim to quickly localize the relative location of the target range in low resolution of the video by downsampling, and then refine the accurate boundaries in the decoder part when upsampling to the original resolution. Inspired by the observations above, we propose a Multi-Resolution Temporal Network (MRTNet) for the video sentence grounding task to simultaneously address all the above-mentioned limitations. It mainly consists of a multi-modal feature encoder, a multi-resolution temporal (MRT) module, and a predictor module. Our MRT model is hot-pluggable, and can be seamlessly incorporated into any stronger proposal-free or proposal-based video sentence grounding network. Besides, we utilize a vision-and-linguistic Transformer to encode the multi-modal features with attention. Moreover, we propose a novel hybrid loss that fuses Cross Entropy (CE) loss, Structural Similarity Index Measure (SSIM) loss, and Intersection over Union (IoU) loss to supervise the training process of accurate video sentence grounding in three levels: frame-level, clip-level, and sequence-level. We demonstrate the effectiveness of the proposed MRTNet on multiple benchmarks. From the experimental results and ablation study, we observe consistent improvements across extensive ablations and settings.

In summary, our proposed MRTNet has the following advantages:

- We propose a novel multi-resolution temporal video sentence grounding network: MRTNet, which mainly consists of a multi-modal feature encoder, a multi-resolution temporal (MRT) module, and a predictor module. We use a multi-modal transformer to encode the visual and linguistic features. Our MRT model is hot-pluggable, and can be seamlessly incorporated into any stronger proposal-free or proposal-based video sentence grounding network.
- We propose a hybrid loss that fuses CE loss, SSIM loss, and IoU loss to supervise the training process of accurate video sentence grounding in three levels: frame-level, clip-level, and sequence-level.
- Experimental results show that our MRT module can effectively improve the performance of different baseline methods in terms of popular evaluation metrics.

2 RELATED WORK

2.1 Video Sentence Grounding

Video sentence grounding is defined as retrieving video segments corresponding to language queries [1, 20, 21, 41]. Most proposed methods [16, 22] treat this task as a ranking problem. They first generate a certain amount of proposals of video segments, and then match the visual content of proposals and linguistic information of language queries. After ranking segment proposals according to the multi-modal matching, the best matching moment for the query can be selected. Similar to object detection, which also generates proposals first and then classifies the content in the bounding box, mining appropriate numbers of positive and negative samples are important for model performance. Thus, many methods always densely sample video moment proposals to achieve good performance, which leads to large computation costs.

To overcome the above-mentioned drawbacks, [49] propose a proposal-free method, which utilizes a Bi-LSTM to encode visual and sentence features, and a co-attention interaction module to fuse

multi-modal features. The model treats the video as a whole and directly predicts the temporal coordinates according to the sentence queries. [24] propose a dense bottom-up framework, which treats all frames corresponding to the language query as foreground, and then regresses the unique distances of each frame in the foreground to bi-directional ground-truth boundaries, finally fuses appropriate temporal candidates as final result. To mine the relationship of sentence semantics with diverse video contents, Yuan et al. [48] also propose a semantic conditioned dynamic modulation, which leverages sentence semantic information to modulate the temporal convolution processes in a hierarchical temporal convolutional network, and establishes a precise matching relationship between sentence and video. Recently, [54] propose a 2D temporal map to model the temporal relations of different moments with variant length, in which the two dimensions indicate the start and end timestamps, respectively. Apart from these top-down and bottom-up methods, there are also works [35] [15] which adopt reinforcement learning to make decisions on the action space of candidate segments, such as the start or end boundaries move left or right, corresponding to the language query matching result.

Among previous works, most similar to ours is DRN [50].

They propose a dense regression network with three different heads to generate accurate boxes. However, directly training three head branches is difficult and unstable, the authors propose a three-step strategy to train the proposed DRN [50]. Different from generating candidate boxes in different scales, we propose a multi-resolution temporal network to further leverage the benefit of 1D temporal attention to better model the context information in different resolutions, which improves a lot for the accurate temporal region in videos. Besides, to obtain accurate attention information, we utilize a hybrid loss to regularize the attention map from three different levels respectively. Furthermore, our proposed module can be plugged into other anchor-free baselines and can be easily trained in an end-to-end manner.

2.2 Multi-modal Transformer

Transformer [34] is first proposed in natural language processing community, which consists of the encoder and decoder with self-attention to deal with the neural machine translation problem. Then, transformer-based networks are proposed to deal with various NLP tasks, such as language modeling [8], word sense disambiguation [33], and learning sentence representations [9]. Due to the great success of Transformer in NLP tasks, its applications to vision tasks have received increasing attention [10]. By splitting the image into fixed-size patches, an image can be treated as a sequence of vectors, which is the same as a sentence. Visual Transformer can be applied in a series of CV tasks, such as image classification [37], semantic segmentation [36], etc.

As for the multimedia area, several works have tried to utilize Transformer architecture to deal with the multi-modal feature interaction. For example, [11] propose a multi-modal transformer to jointly encode the different modalities in video, so as to retrieve the corresponding video according to language and audio. [46] propose a Multi-modal Transformer model for image captioning, which simultaneously captures intra-modal and inter-modal interactions in a

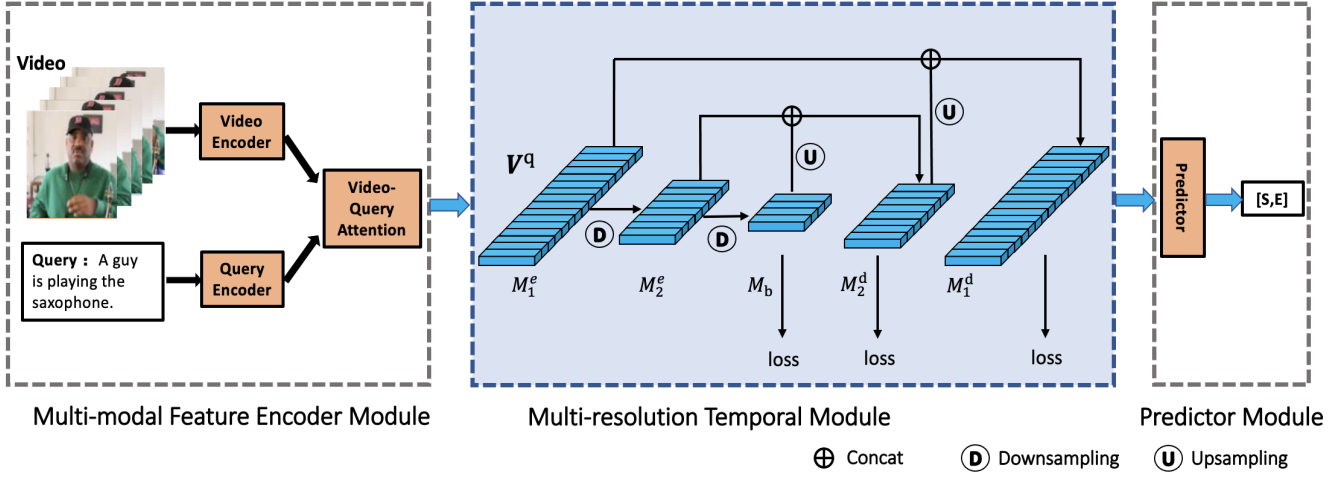


Figure 2: The overview architecture of the MRTNet model, which consists of three parts, including Multi-modal Feature Encoder Module, Multi-resolution Temporal Module, and Predictor Module. Taking the untrimmed video and language query as input, the Feature Encoder Module first extracts the video and query feature by Video Encoder and Query Encoder separately. Then cross-modal features are fused by video-query attention mechanism. Taking the cross-modal features as input, multi-resolution temporal module use an encoder-decoder architecture with downsampling and upsampling, and regularizes the context temporal information from different resolutions. Finally, the temporal boundary results (start and end timestamps) are predicted according to the temporal context-aware features.

unified attention block. In this paper, we propose to use Transformers to encode the multi-modal features and predict the start and end timestamps.

3 APPROACH

In this paper, we propose an MRTNet model to deal with the video sentence grounding task. To sum up, MRTNet mainly consists of three parts: multi-modal feature encoder module, multi-resolution temporal module, and a predictor module. The whole architecture of MRTNet is illustrated in Figure 2. In this section, we first define the problem formulation and describe the multi-modal feature encoder module. Then, we present the details of the Multi-Resolution Temporal (MRT) module. Finally, we calculate the start and end timestamps in the predictor module and show the training and inference processes of MRTNet in detail.

3.1 Problem Formulation

Given an untrimmed video $V = [f_t]_{t=1}^T$ and the language query $Q = [q_j]_{j=1}^M$, where T and M are the numbers of frames and words, respectively, our goal is to predict the start and end timestamp (τ^s, τ^e) in the video corresponding to query Q . For each video V , we extract its visual features $V = [v_i]_{i=1}^n$ with a pretrained 3D ConvNet, where n is the length of extracted features, each feature v_i here is a video feature vector. For each query Q , we initialize the word features $Q = [q_j]_{j=1}^m$ by using GloVe embeddings.

3.2 Multi-modal Feature Encoder Module

For the visual feature $V \in \mathbb{R}^{n \times d_v}$ and linguistic feature $Q \in \mathbb{R}^{m \times d_q}$, We first project them into the same dimension d by two linear layers. Then we adopt the same embedding encoder layer as QANet [44] to

build the visual and linguistic feature encoder, which consists of four convolution layers, a multi-head attention layer [34], a layer normalization layer, and a feed-forward layer with the residual connection. The encoded visual features and query features are as follows:

$$\begin{aligned} \tilde{V} &= \text{VisualEncoder}(VW^v), \\ \tilde{Q} &= \text{QueryEncoder}(QW^q) \end{aligned} \quad (1)$$

where W^v and W^q are projection matrices to keep the dimension consistency between two modalities. The parameters of feature encoder are shared by two modal features.

Multi-modal Attention. With the encoded visual and query features, we calculate the similarity of two modal features and fuse the multi-modal features by a multi-modal attention mechanism. Similar to [24], we first calculate the similarity scores, $\mathcal{S} \in \mathbb{R}^{n \times m}$, between each visual feature and query feature. Then the attention weights of visual-to-query (\mathcal{A}) and query-to-visual (\mathcal{B}) are computed as:

$$\begin{aligned} \mathcal{A} &= \mathcal{S}_r \cdot \tilde{Q} \in \mathbb{R}^{n \times d}, \\ \mathcal{B} &= \mathcal{S}_r \cdot \mathcal{S}_c^T \cdot \tilde{V} \in \mathbb{R}^{n \times d}, \end{aligned} \quad (2)$$

where \mathcal{S}_r and \mathcal{S}_c are the row-wise and column-wise normalization of \mathcal{S} by softmax operation, respectively. Finally, the output of visual-query attention is written as:

$$V^q = \text{FFN}([\tilde{V}; \mathcal{A}; \tilde{V} \odot \mathcal{A}; \tilde{V} \odot \mathcal{B}]), \quad (3)$$

where $V^q \in \mathbb{R}^{n \times d}$; FFN is a single feed-forward layer; \odot denotes element-wise multiplication. V^q is the fused multi-modal semantic features with visual and query attention.

3.3 Multi-Resolution Temporal Module

The multi-modal features V^q we obtain above are in the same length as the video feature V . However, the temporal consistency of video sequence in different resolutions lacks of exploration. Inspired by the U-Net [29], we design a multi-resolution temporal module in an encoder-decoder fashion. This encoder-decoder design is able to capture global contexts in low resolution and refine accurate temporal boundary information in high resolution at the same time. Both encoder and decoder have three different scales of temporal features.

Specifically, the encoder has two stages with the output from high resolution to low resolution, each stage is comprised of two convolution layers with 128 filters and a non-overlapping max-pooling layer of size 2. To further capture global information in the lowest resolution, we add a bridge stage between the encoder and decoder, which consists of one convolutional layer with 128 dilated (dilation = 2) 3×3 filters. Each of these convolutional layers is followed by a batch normalization [17] and a ReLU activation function, *i.e.*,

$$\begin{aligned} M_2^e &= \text{Pooling}(\text{Conv}(M_1^e)), \\ M_b &= \text{Pooling}(\text{Conv}(M_2^e)). \end{aligned} \quad (4)$$

where M_1^e , M_2^e represents the multi-modal features in encoder part, here M_2^e is the same value as V^q . Here we use the depth-wise convolution for efficient network structure. More choice about the encoder layer is discussed in Section 7.

Then, the concentrated video feature in the lowest resolution (*i.e.*, M_b) are concatenated with language feature \tilde{Q} again. To make the length of language and visual feature consistent, we use an weighted pooling on the language feature \tilde{Q} , *i.e.*,

$$M_b = \text{FFN}([\text{Pooling}(W_m M_b), \text{Pooling}(W_q \tilde{Q})]), \quad (5)$$

For decoder, we try to refine the accurate boundaries of responding region while recovering to high resolution. Specifically, decoder is almost symmetrical to the encoder. There are also two corresponding stages with the output from low resolution to high resolution in the decoder design. Each stage consists of two convolution layers followed by a batch normalization and a ReLU activation function, *i.e.*,

$$\begin{aligned} M_2^d &= \text{Conv}([\text{UpPooling}(M_b), M_2^e]), \\ M_1^d &= \text{Conv}([\text{UpPooling}(M_2^d), M_1^e]). \end{aligned} \quad (6)$$

The input of each stage is the concatenated feature maps of the up-sampled output from its previous stage and its corresponding stage in the encoder. In total, there are features in three different resolutions among the multi-resolution temporal modules. To fully supervise the generated temporal features in different resolutions, the output of each decoder block is supervised by the ground-truth temporal labels in their corresponding resolutions. To be specific, the ground-truth temporal labels can be transferred as 1D temporal maps G : The length of the whole video can be divided as n clips (*e.g.*, 128 clips), and all clips lie in the corresponding region of the query are represented as 1, the other clips are 0.

The multi-channel output of the bridge stage and each decoder stage is fed to a plain 3×3 convolution layer followed by a bilinear upsampling and a sigmoid function. Therefore, given an input temporal feature, our prediction module produces three temporal attention maps of different resolutions in the training process. To

obtain the 1D temporal maps of result, we use an 1D convolution layer with kernel of 3×3 to output the features with one channel. Although each predicted map is upsampled to the same size with the input video length, the last one M_2^d has the highest accuracy and hence is taken as the final input of the prediction module.

3.4 Predictor Module

We follow [53] and construct a predictor by using two unidirectional LSTMs to predict the start and end logits according to feature M_1^d . Meanwhile, two LSTMs are stacked so that prediction of end boundaries can be conditioned on those of start boundaries:

$$\begin{aligned} S_t^s &= \mathbf{W}_s \times ([\text{UniLSTM}_{\text{start}}(M_1^d, h_{t-1}^s); M_1^d]) + \mathbf{b}_s, \\ S_t^e &= \mathbf{W}_e \times ([\text{UniLSTM}_{\text{end}}(S_t^s, h_{t-1}^e); M_1^d]) + \mathbf{b}_e. \end{aligned} \quad (7)$$

Here, S_t^s and S_t^e denote the scores of start and end boundaries at position t ; v_t^q represents the t -th feature in V^q .

Then, the probability distributions of start and end boundaries ($P_s \in \mathbb{R}^n$, $P_e \in \mathbb{R}^n$) are calculated by:

$$\begin{aligned} P_s &= \text{Softmax}(S^s), \\ P_e &= \text{Softmax}(S^e), \end{aligned} \quad (8)$$

Inference. Suppose the video duration is \mathcal{T} , the start (end) index is calculated by $a^{s(e)} = \lceil \tau^{s(e)} / \mathcal{T} \times n \rceil$, where $\lceil \cdot \rceil$ denotes the rounding operator. During the inference, the predicted boundary can be easily converted to the corresponding time via $\hat{\tau}^{s(e)} = \hat{a}^{s(e)} / n \times \mathcal{T}$, and the predicted moment locations (\hat{a}^s , \hat{a}^e) of a query is generated by maximizing the joint probability of start and end boundaries by:

$$\begin{aligned} (\hat{a}^s, \hat{a}^e) &= \arg \max_{\hat{a}^s, \hat{a}^e} P_s(\hat{a}^s) P_e(\hat{a}^e) \\ \text{s.t. } 0 \leq \hat{a}^s \leq \hat{a}^e \leq n \end{aligned} \quad (9)$$

3.5 Hybrid Loss

To fully supervise the generated temporal features M_2^d , M_1^d , and M_b in different resolutions, our training loss of multi-resolution temporal module is defined as the summation over all outputs, *i.e.*,

$$\mathcal{L} = \sum_{k=1}^K \alpha_k \ell^{(k)}, \quad (10)$$

where $\ell^{(k)}$ denotes the loss of the k -th 1D temporal features, K denotes the total number of the outputs and α_k is the weight of each loss. In our experiments, MRTNet is deeply supervised with outputs in three resolutions, *i.e.*, $K = 3$.

In each $\ell^{(k)}$, we propose to define $\ell^{(k)}$ as a hybrid loss to obtain high quality temporal location and clear boundaries:

$$\ell^{(k)} = \ell_{ce}^{(k)} + \ell_{ssim}^{(k)} + \ell_{iou}^{(k)}, \quad (11)$$

where $\ell_{ce}^{(k)}$, $\ell_{ssim}^{(k)}$, and $\ell_{iou}^{(k)}$ denote CE loss, SSIM loss and IoU loss, respectively.

CE loss is widely-used in previous video sentence grounding methods. It is defined as:

$$L_{ce} = \frac{1}{2} [L_{ce}(P_s, Y_s) + L_{ce}(P_e, Y_e)], \quad (12)$$

where L_{ce} represents cross-entropy loss function; Y_s and Y_e are the labels for the start (a^s) and end (a^e) boundaries, respectively. P_s and P_e are generated according to Eq. 8.

SSIM (Structural Similarity Index Measure) loss [38], is originally devised for image quality assessment. It captures the structural

Table 1: Statistics of Charades-STA, ActivityNet Caption, and TACoS datasets.

Dataset	Charades-STA	ActivityNet Captions	TACoS
Source	Homes	YouTube	Lab Kitchen
Domain	Indoor Activity	Open	Kitchen Cooking
#Video	6,672	14,926	1,27
#Annotation	16,128	71,957	18,818
#Moments	11,767	71,957	3,290
Vocabulary Size	1,303	15,505	1,344
Average Video Length (seconds)	30.60	117.60	286.59
Average Moment Length (seconds)	8.09	37.14	6.10
Average Query Length (words)	7.22	14.41	10.05
Annotation Split (Training/ Validation/ Testing)	12,408 / - / 3,720	37,421 / 17,505 / 17,031	10,146 / 4,589 / 4,083

information in an image. Hence, we integrated it into our training loss to learn the structural information of the ground-truths. Let $\mathbf{x} = \{x_j | j = 1, \dots, N\}$ and $\mathbf{y} = \{y_j | j = 1, \dots, N\}$ be the pixel values of two corresponding clips (size: $1 \times N$) cropped from the predicted probability map S and the binary 1D temporal GT mask G , respectively. The SSIM loss of \mathbf{x} and \mathbf{y} is calculated as followed:

$$L_{ssim} = 1 - \frac{(2\mu_x\mu_y + C_1)(2\sigma_{xy} + C_2)}{(\mu_x^2 + \mu_y^2 + C_1)(\sigma_x^2 + \sigma_y^2 + C_2)} \quad (13)$$

where μ_x , μ_y and σ_x , σ_y are the mean and standard deviations of \mathbf{x} and \mathbf{y} , respectively, σ_{xy} is covariance. $C_1 = 0.01^2$ and $C_2 = 0.03^2$ are used to avoid dividing by 0.

IoU loss is originally proposed for measuring the similarity between two sets and has become a standard evaluation measure for object detection and segmentation. Recently, it has been used as a training loss. To ensure its differentiability, we adopted the IoU loss used in [25], *i.e.*,

$$L_{iou} = 1 - \frac{\sum_{c=1}^W S(c)G(c)}{\sum_{c=1}^W [S(c)+G(c)-S(c)G(c)]}, \quad (14)$$

where $G(c) \in \{0, 1\}$ is the GT label of the pixel c and $S(c)$ is the predicted probability of 1D temporal map.

To take advantage of the above three losses, we combine them together to compose the hybrid loss. CE is used to maintain a smooth gradient for all pixels, while IoU is employed to put more focus on the foreground. SSIM is used to encourage the prediction to respect the structure of the original image, by employing a larger loss near the boundaries, as well as further make the predictions of the background close to zero.

4 EXPERIMENTS

4.1 Datasets

To evaluate the performance of our proposed MRTNet, we conduct experiments on three challenging video sentence grounding datasets:

- **Charades-STA** [12] is composed of daily indoor activities videos, which is based on Charades dataset [32]. This dataset contains 6672 videos, 16,128 annotations, and 11,767 moments. The average length of each video is 30 seconds. 12,408 and 3,720 moment annotations are labeled for training and testing, respectively;

- **ActivityNet Caption** [2] is originally constructed for dense video captioning, which contains about 20k YouTube videos with an average length of 120 seconds. As a dual task of dense video captioning, video sentence grounding utilize the sentence description as query and output the temporal boundary of each sentence description.
- **TACoS** [28] is collected from MPII Cooking dataset [28], which has 127 videos with an average length of 286.59 seconds. TACoS has 18,818 query-moment pairs, which are all about cooking scenes. We follow the same splits in [12], where 10,146, 4,589 and 4,083 annotations are used for training, validation and test, respectively.

The details of each dataset are summarized in Table 1. It is worth noting that some methods make minor changes to the dataset when evaluating the experimental performance. For example, CMIN [55] uses val_1 as validation set and val_2 as testing set in the ActivityNet Captions dataset, while other methods [54] combine the val_1 and val_2 together as the testing set. And for TACoS dataset, 2DTAN [54] utilize a modified TACoS dataset for evaluation. To make a fair comparison, we follow the setting of dataset splitting report in their original papers when evaluating the performance of our method.

4.2 Evaluation Metrics

Following existing video grounding works, we evaluate the performance on two main metrics:

mIoU: “mIoU” is the average predicted Intersection over Union over all testing samples. The mIoU metric is particularly challenging for short video moments;

Recall: We adopt “R@ n , IoU = μ ” as the evaluation metrics, following [12]. The “R@ n , IoU = μ ” represents the percentage of language queries having at least one result whose IoU between top- n predictions with ground-truth is larger than μ . In our experiments, we reported the results of $n = 1$ and $\mu \in \{0.3, 0.5, 0.7\}$.

4.3 Implementation Details

For language query Q , we use the 300-D GloVe [27] vectors to initialize each lowercase word, and these word embeddings are fixed during training. For video V , we downsample frames and extract RGB visual features using the 3D ConvNet which was pre-trained on the Kinetics dataset. We set the dimension of all the hidden layers in the model as 128, the kernel size of the convolutional layer as

Table 2: Performance comparison (%) with the state-of-the-art models on TACoS dataset. Noted that the improvement achieved by MRTNet is significant.

Methods	R@1,IoU=0.3	R@1,IoU=0.5	R@1,IoU=0.7	mIoU
CTRL ICCV2017	18.32	13.30	—	—
ACRN SIGIR 2018	19.52	14.62	—	—
MCF IJCAI2018	18.64	—	—	—
SM-RL CVPR2019	20.25	15.95	—	—
ACL WACV2019	22.07	17.78	—	—
SAP AAAI2019	—	18.24	—	—
L-NET AAAI2019	—	—	—	13.41
TGN EMNLP2018	21.77	18.90	—	—
ABLR-aw AAAI2019	18.90	9.30	—	12.50
ABLR-af AAAI2019	19.60	—	—	13.40
DEBUG EMNLP2019	23.45	11.72	—	16.03
CMIN SIGIR2019	24.64	18.05	—	—
GDP AAAI2020	24.14	—	—	16.18
DRN CVPR2020	—	23.17	—	—
SeqPAN ACL2021	31.72	27.19	21.65	25.86
VSLNet ACL2020	29.61	24.27	20.03	24.11
MRTNet (VSLNet)	32.35	25.84	21.31	26.14
2D-TAN AAAI2020	37.29	25.32	13.32	25.19
MRTNet (2D-TAN)	37.81	26.01	14.95	26.29

7, and the head size of multi-head attention as 8. For all datasets, models were trained for 100 epochs. The batch size was set to 16. Dropout and an early stopping strategies were adopted to prevent overfitting. The whole framework was trained by Adam optimizer with an initial learning rate 0.0001.

Table 3: Performance comparison (%) with the state-of-the-art models on ActivityNet Captions dataset. Noted that the improvement achieved by MRTNet is significant.

Methods	R@1,IoU=0.3	R@1,IoU=0.5	R@1,IoU=0.7	mIoU
CMIN SIGIR2019	63.61	43.40	23.88	—
TGN EMNLP2018	43.81	27.93	—	—
QSPN AAAI2019	45.30	27.70	13.60	—
RWM AAAI2019	—	36.90	—	—
ABLR-af AAAI2019	53.65	34.91	—	35.72
ABLR-aw AAAI2019	55.67	36.79	—	36.99
DEBUG EMNLP2019	55.91	39.72	—	39.51
GDP AAAI2020	56.17	39.27	—	39.80
DRN CVPR2020	58.52	41.51	23.07	41.13
CI-MHA SIGIR2021	61.49	43.97	25.13	—
SeqPAN ACL2021	61.65	45.50	29.37	45.11
VSLNet ACL2020	63.16	43.22	26.16	43.19
MRTNet (VSLNet)	64.17	44.09	27.43	44.82
2D-TAN AAAI2020	59.45	44.51	27.38	43.29
MRTNet (2D-TAN)	60.71	45.59	28.07	44.54

4.4 Comparison with State-of-the-Arts

4.4.1 Experimental Settings. We compare our proposed MRTNet with state-of-the-art video sentence grounding methods on three public datasets. These methods can be grouped into three categories

Table 4: Performance (%) comparison with the state-of-the-art models on Charades-STA dataset. Noted that the improvement achieved by MRTNet is significant.

Methods	R@1,IoU=0.3	R@1,IoU=0.5	R@1,IoU=0.7	mIoU
CTRL ICCV2017	—	23.63	8.89	—
ROLE MM2018	25.26	12.12	—	—
ACL WACV2019	—	30.48	12.20	—
SAP AAAI2019	—	27.42	13.36	—
RWM AAAI2019	—	36.70	—	—
SM-RL CVPR2019	—	24.36	11.17	—
QSPN AAAI2019	54.70	35.60	15.80	—
DEBUG EMNLP2019	54.95	37.39	17.92	36.34
GDP AAAI2020	54.54	39.47	18.49	—
DRN CVPR2020	—	42.90	23.68	41.28
ExCL ACL2019	—	44.10	22.40	—
MAN CVPR2019	—	46.53	22.72	—
CI-MHA SIGIR2021	69.87	54.68	35.27	—
VSLNet ACL2020	70.46	54.19	35.22	50.02
MRTNet (VSLNet)	70.88	56.19	36.37	50.74
2D-TAN AAAI2020	57.31	42.80	23.25	39.23
MRTNet (2D-TAN)	59.23	44.27	25.88	40.59

according to the viewpoints of proposal-based, proposal-free, and other approaches:

1) Proposal-based models: **CTRL** [12], **ACRN** [22], **ROLE** [23], **MCF** [39], **ACL** [13], **SAP** [6], **QSPN** [42], **CMIN** [55] **TGN** [3], **2D-TAN** [54] **MAN** [51]; 2) Proposal-free models: **L-Net** [4], **ABLR-aw** [49], **ABLR-af** [49], **DEBUG** [24], **CI-MHA** [47] **ExCL** [14], **GDP** [5], **VSLNet** [53], **LGI** [26], **DRN** [50] **SeqPAN** [52]; 3) Others: **RWM** [15], **SM-RL** [35].

4.4.2 Quantitative Results. The results on three benchmarks are reported from Table 2 to Table 4, respectively. According to the experimental results, we can observe that our MRTNet can effectively improve the performance of baseline networks over all metrics and benchmarks. We choose VSLNet [53] and 2D-TAN [54] as baseline networks, which are known as typical proposal-free and proposal-based models with published source codes.

- For the implementation based on each baseline method, our MRTNet (VSLNet) shares the same architecture as VSLNet in Feature Encoder Module. Specifically, we implement the VSLNet with C3D feature followed the settings they reported in original paper. VSLNet extracts the frame-level feature using the backbone of QANet [45] and utilizes two LSTMs to classify the start and end boundary. For the MRTNet (2D-TAN), we add the MRT Module before restructuring the 2D temporal feature map. For other modules in each baseline network, we follow the same settings according to original papers.
- Table 4 summarizes the experimental results on Charades-STA dataset. We can observe that MRTNet (VSLNet) works well in even stricter metrics, e.g., MRTNet (VSLNet) achieves a significant 1.28% absolute improvement in IoU@0.7 and MRTNet (2D-TAN) achieves 1.63% absolute improvement in IoU@0.7, which demonstrates the effectiveness of proposed model. It is mainly because that MRTNet better utilizes

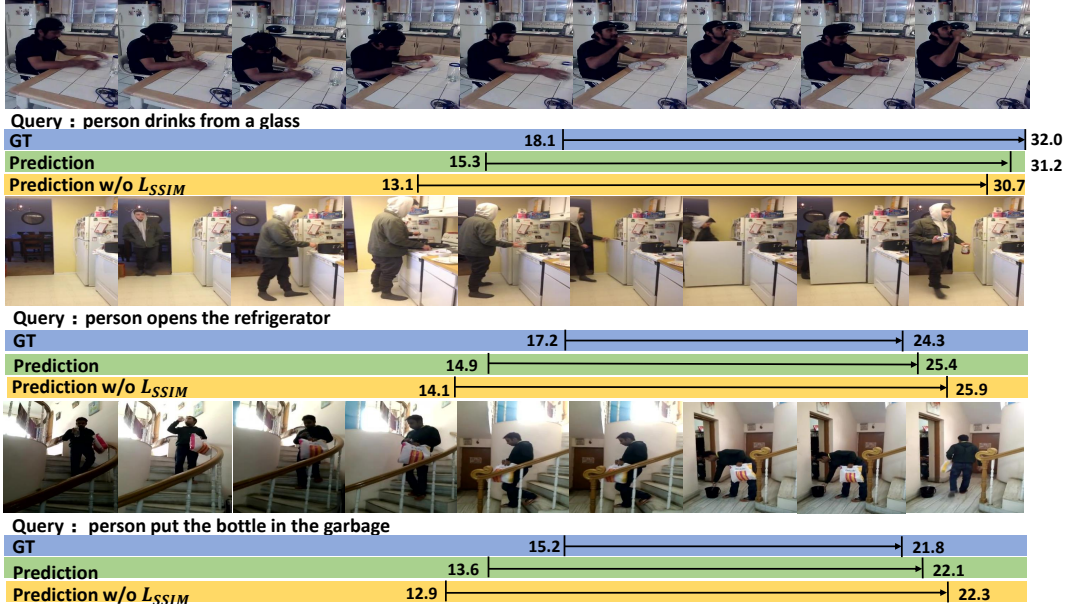


Figure 3: Qualitative results of MRTNet (VSLNet) on Charades-STA dataset.

the temporal consistency of video sequences in different resolutions and utilizes a hybrid loss to better regularize the multi-modal features. The results on TACoS and ActivityNet Captions dataset are summarized in Table 2 and Table 3, respectively. Note that videos in TACoS have a longer average duration and the ground-truth video segments in ActivityNet Captions have a longer average length. Although there exists bias in the data distribution of datasets [43], MRTNet significantly outperforms the other methods on both benchmarks with the C3D feature, which demonstrates that MRTNet is highly adaptive to videos and segments with diverse lengths, and can bring in consistent improvement based on different baseline methods.

- Our proposed MRT module also has good generalization ability, since the input multi-modal features of the MRT module keep in the same dimension as output features, then this module can be easily plugged into any other proposal-based or proposal-free video grounding network, and the whole network with proposed hybrid loss can be trained in an end-to-end manner.

4.4.3 Qualitative Results. As illustrated in Figure 3, the qualitative results of MRTNet (VSLNet) on Charades-STA dataset are reported. According to the three examples, the localized moments generated by MRTNet are very close to ground-truth. If we train the model without SSIM loss, the generated temporal region will be more expansive compared with the ground-truth region, which is shown as a longer temporal interval with high confidence. Hence, the model trained with SSIM loss can better capture the accurate boundaries of query-corresponding temporal regions.

4.5 Ablative Studies

We conduct ablative experiments to analyze the effectiveness of hybrid loss in our approach. Also, we analyze the effectiveness of the MRT module in MRTNet. For simplification, the ablation experiments introduced below are conducted on the TACoS dataset with VSLNet as the baseline.

4.5.1 Multi-resolution Temporal Module. From the results in Figure 4 below, we can observe that three layers in the encoder-decoder structure is the most appropriate setting when dealing with videos of different lengths, which can achieve a trade-off between speed and accuracy.

Table 5: Performance comparison (%) of MRTNet (VSLNet) with different encoding layers on TACoS dataset.

Encoding Layer	R@1, IoU=0.5	R@1, IoU=0.7	mIoU
Convolution	25.84	21.31	26.14
Transformer	25.91	21.14	26.21

Then, we consider replacing the convolution layer with vanilla Transformer in the encoder part of multi-resolution module, as shown in Eq. (4). According to Table 5, we can observe that the performance of using Transformer layer in the encoder part is comparative with using convolution, but causes larger computation cost. To make a trade-off between speed and accuracy, our MRTNet use depth-wise convolution in the encoder layer.

4.5.2 Hybrid Loss. To demonstrate the effectiveness of each component in our proposed hybrid loss, we conduct a set of experiments over different losses based on our MRTNet architecture.

- The CE loss is computed in the frame-level. It mainly evaluates the possibility of two peaks in time dimension: start

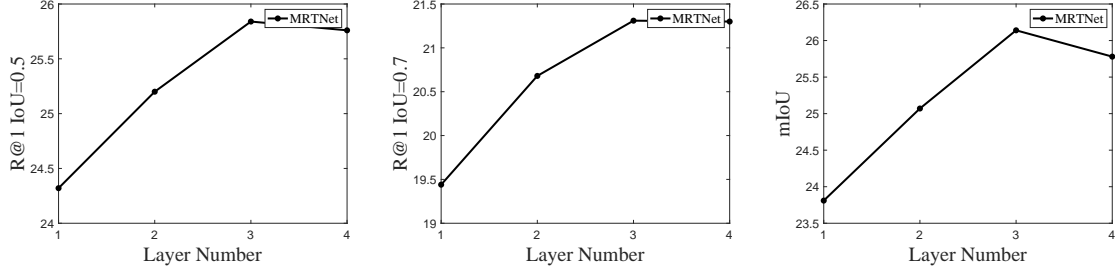


Figure 4: Performance comparison (%) of MRTNet (VSLNet) in different layer numbers on TACoS dataset.

Table 6: Performance comparison (%) of MRTNet (VSLNet) with different losses on TACoS dataset.

Loss	ℓ_{ce}	ℓ_{ssim}	ℓ_{iou}	R@1, IoU=0.7	mIoU
MRT Module	✓			20.01	24.94
	✓	✓		20.30	25.26
	✓		✓	20.24	25.29
	✓	✓	✓	21.31	26.14

and end timestamps. As shown in Table 6, training the MRTNet (VSLNet) model with merely CE loss achieves 24.94 in mIoU.

- The SSIM loss is a clip-level measure, which considers the local neighborhood of each clip. It assigns higher weights to pixels located in the transitional buffer regions between foregrounds and backgrounds, *e.g.* boundaries, so that the loss is higher around the boundary.

Models trained with the SSIM loss are able to predict correct results on the foreground region and boundaries while neglecting the background accuracy at the beginning of the training process. The results in Table 6 indicate that the proposed SSIM loss greatly improves the performance, which brings about 0.7% performance gain on average in the metric of mIoU. The SSIM loss can regularize the features at clip-level and refine the temporal boundaries. This characteristic of the SSIM loss helps model to focus on the boundary and foreground region.

- The IoU loss is a sequence-level measure. Models trained with IoU loss emphasize more on the large foreground regions and are thus able to produce relatively homogeneous and higher confident probabilities for these regions. As shown in Table 6, utilizing SSIM loss can bring about 0.3% performance gain in the metric of mIoU.

According to the detailed analysis of each loss, it is clear that our hybrid loss is beneficial to better feature learning and can achieve superior qualitative results.

4.5.3 Computation Complexity. We evaluate the computation complexity of MRTNet compared with other SOTA methods on TACoS dataset.

- According to Table 2 and Table 7, MRTNet achieves better performance compared with baseline methods in all experimental cases. Due to the utilization of depth-wise convolution,

the model size of whole network has only minor increment (almost 6%) compared with the baseline 2D-TAN method.

- We also try to replace the convolution layer in encoder part of MRT Module with vanilla Transformer layer, which can further improve the performance but brings in more parameters and increase the running time.
- The experimental results show that utilizing the characteristic of multi-resolution in video can bring in steady improvement based on each baseline network and still have potential for better performance. To be specific, we can use light-weighted version convolution or Transformer layers to achieve better performance while relieving the burden of computation cost. Also, there also exists a series of variants designed for multi-scale feature interaction, such as pyramid pooling, multi-scale attention, and so on.

Table 7: Computation Complexity Comparison with SOTA methods on TACoS dataset.

Method	Running Time	Model Size	R@1, IoU=0.5
CTRL	2.23s	22M	13.30
ACRN	4.31s	128M	14.62
TGN	0.92s	166M	18.90
DRN	0.15s	214M	23.17
2D-TAN	0.57s	232M	25.32
MRTNet (2D-TAN) +Transformer	0.68s 0.82s	249M 284M	26.01 26.21

5 CONCLUSION

In this work, we propose a novel multi-resolution temporal video sentence grounding network: MRTNet, which mainly consists of a multi-model feature encoder, a Multi-Resolution Temporal (MRT) module, and a predictor. Our MRT module is plug-and-play, which means it can be seamlessly incorporated into any video sentence grounding baseline network. Besides, we propose a hybrid loss to supervise the cross-modal features of accurate video sentence grounding in three levels: frame-level, clip-level, and sequence-level. Through extensive experiments on three benchmark datasets, we show that MRTNet outperforms the baseline methods; and the proposed MRT module is easy to plug into other video sentence grounding frameworks. In future work, we will explore more efficient and light-weighted models to make quick video sentence grounding inference.

REFERENCES

- [1] Lisa Anne Hendricks, Oliver Wang, Eli Shechtman, Josef Sivic, Trevor Darrell, and Bryan Russell. 2017. Localizing moments in video with natural language. In *ICCV*. 5803–5812.
- [2] Fabian Caba Heilbron, Victor Escorcia, Bernard Ghanem, and Juan Carlos Niebles. 2015. Activitynet: A large-scale video benchmark for human activity understanding. In *CVPR*. 961–970.
- [3] Jingyuan Chen, Xinpeng Chen, Lin Ma, Zequin Jie, and Tat-Seng Chua. 2018. Temporally grounding natural sentence in video. In *EMNLP*. 162–171.
- [4] Jingyuan Chen, Lin Ma, Xinpeng Chen, Zequin Jie, and Jiebo Luo. 2019. Localizing natural language in videos. In *AAAI*, Vol. 33. 8175–8182.
- [5] Long Chen, Chujie Lu, Siliang Tang, Jun Xiao, Dong Zhang, Chilie Tan, and Xiaolin Li. 2020. Rethinking the bottom-up framework for query-based video localization. In *AAAI*, Vol. 34. 10551–10558.
- [6] Shaoliang Chen and Yu-Gang Jiang. 2019. Semantic proposal for activity localization in videos via sentence query. In *AAAI*, Vol. 33. 8199–8206.
- [7] Yun-Wei Chu, Kuan-Yen Lin, Chao-Chun Hsu, and Lun-Wei Ku. 2021. End-to-end Recurrent Cross-Modality Attention for Video Dialogue. *TASLP* (2021).
- [8] Zihang Dai, Zhilin Yang, Yiming Yang, William W Cohen, Jaime Carbonell, Quoc V Le, and Ruslan Salakhutdinov. 2018. Transformer-xl: Language modeling with longer term dependency. (2018).
- [9] Jacob Devlin, Ming-Wei Chang, Kenton Lee, and Kristina Toutanova. 2018. Bert: Pre-training of deep bidirectional transformers for language understanding. *arXiv preprint arXiv:1810.04805* (2018).
- [10] Alexey Dosovitskiy, Lucas Beyer, Alexander Kolesnikov, Dirk Weissenborn, Xiaohua Zhai, Thomas Unterthiner, Mostafa Dehghani, Matthias Minderer, Georg Heigold, Sylvain Gelly, et al. 2020. An image is worth 16x16 words: Transformers for image recognition at scale. *arXiv preprint arXiv:2010.11929* (2020).
- [11] Valentin Gabeur, Chen Sun, Kartek Alahari, and Cordelia Schmid. 2020. Multi-modal transformer for video retrieval. In *ECCV*, Vol. 5. Springer.
- [12] Jiyang Gao, Chen Sun, Zhenheng Yang, and Ram Nevatia. 2017. Tall: Temporal activity localization via language query. In *ICCV*. 5267–5275.
- [13] Runzhou Ge, Jiyang Gao, Kan Chen, and Ram Nevatia. 2019. Mac: Mining activity concepts for language-based temporal localization. In *WACV*. 245–253.
- [14] Soham Ghosh, Anuva Agarwal, Zarana Parekh, and Alexander Hauptmann. 2019. Excl: Extractive clip localization using natural language descriptions. *arXiv preprint arXiv:1904.02755* (2019).
- [15] Dongliang He, Xiang Zhao, Jizhou Huang, Fu Li, Xiao Liu, and Shilei Wen. 2019. Read, watch, and move: Reinforcement learning for temporally grounding natural language descriptions in videos. In *AAAI*, Vol. 33. 8393–8400.
- [16] Lisa Anne Hendricks, Oliver Wang, Eli Shechtman, Josef Sivic, Trevor Darrell, and Bryan Russell. 2018. Localizing moments in video with temporal language. *arXiv preprint arXiv:1809.01337* (2018).
- [17] Sergey Ioffe and Christian Szegedy. 2015. Batch normalization: Accelerating deep network training by reducing internal covariate shift. In *ICML*. 448–456.
- [18] Wei Ji, Yicong Li, Meng Wei, Xindi Shang, Junbin Xiao, Tongwei Ren, and Tat-Seng Chua. 2021. VidVRD 2021: The Third Grand Challenge on Video Relation Detection. In *Proceedings of the 29th ACM International Conference on Multimedia*. 4779–4783.
- [19] Yicong Li, Xiang Wang, Junbin Xiao, Wei Ji, and Tat-Seng Chua. 2022. Invariant grounding for video question answering. In *Proceedings of the IEEE/CVF Conference on Computer Vision and Pattern Recognition*. 2928–2937.
- [20] Daizong Liu, Xiaoye Qu, Jianfeng Dong, Pan Zhou, Yu Cheng, Wei Wei, Zichuan Xu, and Yulai Xie. 2021. Context-aware biaffine localizing network for temporal sentence grounding. In *Proceedings of the IEEE/CVF Conference on Computer Vision and Pattern Recognition*. 11235–11244.
- [21] Daizong Liu, Xiaoye Qu, Xiao-Yang Liu, Jianfeng Dong, Pan Zhou, and Zichuan Xu. 2020. Jointly cross- and self-modal graph attention network for query-based moment localization. In *Proceedings of the 28th ACM International Conference on Multimedia*. 4070–4078.
- [22] Meng Liu, Xiang Wang, Liqiang Nie, Xiangnan He, Baoquan Chen, and Tat-Seng Chua. 2018. Attentive moment retrieval in videos. In *SIGIR*. 15–24.
- [23] Meng Liu, Xiang Wang, Liqiang Nie, Qi Tian, Baoquan Chen, and Tat-Seng Chua. 2018. Cross-modal moment localization in videos. In *ACM Multimedia*. 843–851.
- [24] Chujie Lu, Long Chen, Chilie Tan, Xiaolin Li, and Jun Xiao. 2019. DEBUG: A dense bottom-up grounding approach for natural language video localization. In *EMNLP*. 5147–5156.
- [25] Gellért Mátyus, Wenjie Luo, and Raquel Urtasun. 2017. Deeproadmapper: Extracting road topology from aerial images. In *ICCV*. 3438–3446.
- [26] Jonghwan Mun, Minsu Cho, and Bohyung Han. 2020. Local-Global Video-Text Interactions for Temporal Grounding. In *CVPR*. 10810–10819.
- [27] Jeffrey Pennington, Richard Socher, and Christopher D Manning. 2014. Glove: Global vectors for word representation. In *EMNLP*. 1532–1543.
- [28] Michaela Regneri, Marcus Rohrbach, Dominikus Wetzel, Stefan Thater, Bernt Schiele, and Manfred Pinkal. 2013. Grounding action descriptions in videos. *ACL* 1 (2013), 25–36.
- [29] Olaf Ronneberger, Philipp Fischer, and Thomas Brox. 2015. U-net: Convolutional networks for biomedical image segmentation. In *MICCAI*. 234–241.
- [30] Xindi Shang, Yicong Li, Junbin Xiao, Wei Ji, and Tat-Seng Chua. 2021. Video visual relation detection via iterative inference. In *Proceedings of the 29th ACM International Conference on Multimedia*. 3654–3663.
- [31] Xindi Shang, Tongwei Ren, Jingfan Guo, Hanwang Zhang, and Tat-Seng Chua. 2017. Video visual relation detection. In *ACM Multimedia*. 1300–1308.
- [32] Gunnar A Sigurdsson, Güray Varol, Xiaolong Wang, Ali Farhadi, Ivan Laptev, and Abhinav Gupta. 2016. Hollywood in homes: Crowdsourcing data collection for activity understanding. In *ECCV*. 510–526.
- [33] Gongbo Tang, Mathias Müller, Annette Rios, and Rico Sennrich. 2018. Why self-attention? a targeted evaluation of neural machine translation architectures. *arXiv preprint arXiv:1808.08946* (2018).
- [34] Ashish Vaswani, Noam Shazeer, Niki Parmar, Jakob Uszkoreit, Llion Jones, Aidan N Gomez, Łukasz Kaiser, and Illia Polosukhin. 2017. Attention is all you need. *arXiv preprint arXiv:1706.03762* (2017).
- [35] Weining Wang, Yan Huang, and Liang Wang. 2019. Language-driven temporal activity localization: A semantic matching reinforcement learning model. In *CVPR*. 334–343.
- [36] Wenhui Wang, Enze Xie, Xiang Li, Deng-Ping Fan, Kaitao Song, Ding Liang, Tong Lu, Ping Luo, and Ling Shao. 2021. Pyramid vision transformer: A versatile backbone for dense prediction without convolutions. *arXiv preprint arXiv:2102.12122* (2021).
- [37] Wenxiao Wang, Lu Yao, Long Chen, Deng Cai, Xiaofei He, and Wei Liu. 2021. CrossFormer: A Versatile Vision Transformer Based on Cross-scale Attention. *arXiv preprint arXiv:2108.00154* (2021).
- [38] Zhou Wang, Eero P Simoncelli, and Alan C Bovik. 2003. Multiscale structural similarity for image quality assessment. In *The Thirty-Seventh Asilomar Conference on Signals, Systems & Computers*, Vol. 2. Ieee, 1398–1402.
- [39] Aming Wu and Yahong Han. 2018. Multi-modal Circulant Fusion for Video-to-Language and Backward. In *IJCAI*, Vol. 3. 8.
- [40] Junbin Xiao, Angela Yao, Zhiyuan Liu, Yicong Li, Wei Ji, and Tat-Seng Chua. 2022. Video as Conditional Graph Hierarchy for Multi-Granular Question Answering. *AAAI*.
- [41] Shaoning Xiao, Long Chen, Songyang Zhang, Wei Ji, Jian Shao, Lu Ye, and Jun Xiao. 2021. Boundary Proposal Network for Two-Stage Natural Language Video Localization. In *Proceedings of the AAAI Conference on Artificial Intelligence*, Vol. 35. 2986–2994.
- [42] Huijuan Xu, Kun He, Bryan A Plummer, Leonid Sigal, Stan Sclaroff, and Kate Saenko. 2019. Multilevel language and vision integration for text-to-clip retrieval. In *AAAI*, Vol. 33. 9062–9069.
- [43] Xun Yang, Fuli Feng, Wei Ji, Meng Wang, and Tat-Seng Chua. 2021. Deconfounded Video Moment Retrieval with Causal Intervention. *arXiv preprint arXiv:2106.01534* (2021).
- [44] Adams Wei Yu, David Dohan, Quoc Le, Thang Luong, Rui Zhao, and Kai Chen. 2018. Fast and accurate reading comprehension by combining self-attention and convolution. In *ICLR*.
- [45] Adams Wei Yu, David Dohan, Minh-Thang Luong, Rui Zhao, Kai Chen, Mohammad Norouzi, and Quoc V Le. 2018. Qanet: Combining local convolution with global self-attention for reading comprehension. *arXiv preprint arXiv:1804.09541* (2018).
- [46] Jun Yu, Jing Li, Zhou Yu, and Qingming Huang. 2019. Multimodal transformer with multi-view visual representation for image captioning. *TCSVT* 30, 12 (2019), 4467–4480.
- [47] Xinli Yu, Mohsen Malmir, Xin He, Jiangning Chen, Tong Wang, Yue Wu, Yue Liu, and Yang Liu. 2021. Cross Interaction Network for Natural Language Guided Video Moment Retrieval. In *SIGIR*.
- [48] Yitian Yuan, Lin Ma, Jingwen Wang, Wei Liu, and Wenwu Zhu. 2019. Semantic conditioned dynamic modulation for temporal sentence grounding in videos. *arXiv preprint arXiv:1910.14303* (2019).
- [49] Yitian Yuan, Tao Mei, and Wenwu Zhu. 2019. To find where you talk: Temporal sentence localization in video with attention based location regression. In *AAAI*, Vol. 33. 9159–9166.
- [50] Runhao Zeng, Haoming Xu, Wenbing Huang, Peihao Chen, Mingkui Tan, and Chuang Gan. 2020. Dense regression network for video grounding. In *CVPR*. 10287–10296.
- [51] Da Zhang, Xiyang Dai, Xin Wang, Yuan-Fang Wang, and Larry S Davis. 2019. Man: Moment alignment network for natural language moment retrieval via iterative graph adjustment. In *CVPR*. 1247–1257.
- [52] Hao Zhang, Aixin Sun, Wei Jing, Liangli Zhen, Joey Tianyi Zhou, and Rick Siow Mong Goh. 2021. Parallel Attention Network with Sequence Matching for Video Grounding. *arXiv preprint arXiv:2105.08481* (2021).
- [53] Hao Zhang, Aixin Sun, Wei Jing, and Joey Tianyi Zhou. 2020. Span-based localizing network for natural language video localization. *ACL* (2020).
- [54] Songyang Zhang, Houwen Peng, Jianlong Fu, and Jiebo Luo. 2020. Learning 2d temporal adjacent networks for moment localization with natural language. In *AAAI*, Vol. 34. 12870–12877.

[55] Zhu Zhang, Zhijie Lin, Zhou Zhao, and Zhenxin Xiao. 2019. Cross-modal interaction networks for query-based moment retrieval in videos. In *Proceedings of the 42nd International ACM SIGIR Conference on Research and Development in Information Retrieval*. 655–664.

[56] Yaoyao Zhong, Wei Ji, Junbin Xiao, Yicong Li, Weihong Deng, and Tat-Seng Chua. 2022. Video Question Answering: Datasets, Algorithms and Challenges. *EMNLP* (2022).